Mechanochemical Approaches to Ceramic Ink Formulation for Digital Fabrication of Solid Oxide Fuel Cells

L. Jay Deiner[1], Alexis Marruffo[2], Thomas L. Reitz[2]; [1]New York City College of Technology (CUNY); Brooklyn, NY/USA; [2]The Air Force Research Laboratory, Propulsion Directorate, Wright-Patterson Air Force Base, OH/USA

Abstract

Four different ink processing protocols were investigated to control the particle size distribution of lab scale batches of inkjet inks used for printing Solid Oxide Fuel Cell (SOFC) anodes. The inks were composed of a mixture of commercial Nickel Oxide (NiO) and Yttria-stabilized Zirconia (YSZ) powders dispersed in organic solvents. Protocols incorporating high energy wet and dry milling using a SPEX 8000 mixer mill were compared to traditional low energy milling/dispersion methods. Brunauer-Emmett-Teller (B.E.T.) surface area measurements were used in conjunction with scanning electron microscopy (S.E.M.) to determine the effects of the milling protocols on the dry powder particle sizes and morphologies. Dynamic light scattering (D.L.S.) was used to measure the particle size distributions of the inks. Low energy dispersion of the NiO and YSZ powders produced an ink with a number weighted particle size distribution peaked ~ 300 nm and a significant tail of particles as large as 1 μm. Adding high energy dry milling or high energy slurry dispersion to the process removed most of the large particle size tail, but the particle size distribution remained peaked at 250 – 300 nm. By combining high energy dry powder milling with high energy slurry dispersion, the main peak in the particle size distribution shifted to 180 nm with minimal particles above 600 nm. These results indicate that the combination of high energy milling and dispersion enable lab scale production of nanoscale NiO/YSZ inks from commercial powders. The protocols developed in this work provide a first step towards the goal of controlling the microstructure of inkjet printed solid oxide fuel cell (SOFC) anodes through control of the ink particle size distribution.

Introduction

Solid oxide fuel cells are a promising technology for large and medium scale power generation[1]. They are particularly attractive because of their relatively high efficiency and fuel flexibility. Also, in contrast to polymer membrane fuel cells, solid oxide fuel cells generally utilize a nickel oxide/yttria-stabilized zirconia (NiO/YSZ) cermet anode catalyst as opposed to more expensive noble metal-based oxidation catalysts.

One challenge in realizing the potential utility of the solid oxide fuel cell is controlling the anode microstructure, particularly the triple phase boundary where hydrogen or other fuel gas meets the nickel catalyst and the O^{2-} ions that are transported through the YSZ[2]. Catalyst particle size, particle size distribution, porosity, and phase mixing impact the anode microstructure, which in turn determines the triple phase boundary length and surface area[3]. Depending on the desired device characteristics, the anode microstructure could, in principle, be manipulated to bias relative contributions of ionic conductivity, electronic conductivity or electrocatalytic activity within discrete ceramic regions. Examples of the connection between anode microstructure and device performance include studies linking electrochemical performance to anode porosity and porosity gradient[4] and studies showing the kinetic effects of compositional grading[5]. Recent studies have shown that it is possible to affect anode performance by attrition milling of the NiO/YSZ catalyst particles prior to tape casting. It is believed that attrition milling changes not only the NiO and YSZ particle sizes, but also the degree of chemical association between the NiO and YSZ[6-7]. These changes are linked to surface chemical interactions between the NiO and YSZ particles.

Inkjet printing, an emerging technology for solid oxide fuel cell fabrication[8-13], holds significant promise as a method to control anode microstructure. In order to use inkjet printing for microstructural control, it is necessary to manipulate the sizes and surface chemistries of the ceramic particles dispersed in the inks. Ideally, for anode printing, one would formulate an array of stable NiO/YSZ inks with varying ratios of NiO and YSZ and with varying particle size distributions. The sequential printing of inks with different compositions and particle sizes would enable functional grading of catalyst composition, particles sizes and porosities. This grading may lead to the highest performance anodes[14].

The production of true nanoscale NiO/YSZ inks (disaggregated particles in the 100 – 200 nm range) is non-trivial and has not yet been successfully achieved with attrition milling[7]. As such, establishment of formulation protocols to produce true nanoscale NiO/YSZ inks is an unmet challenge in the drive to control anode microstructure. The present work endeavors to address this unmet need. Further, it aims to do so using tools typically available to researchers producing lab scale batches of ink. It is hoped that these ink production protocols will enable future studies which connect NiO/YSZ ink particle sizes to anode microstructure and anode microstructure to electrochemical performance. It is also hoped that the protocols designed for inkjet printing of solid oxide fuel cells can be generalized for digital fabrication of other ceramic and electronic devices.

Experimental

Ink Components and Formulations

All experiments were performed using Nickel Oxide (NiO, Nickelous Oxide, Green, Powder, Baker Analyzed Reagent for Electronic Ceramics, J.T. Baker) and Yttria-stabilized Zirconia (YSZ, Tosoh TZ-8YS) particles. The NiO particles were measured in house to have a B.E.T. surface area of 3.8 m^2/g. The YSZ particles were specified by the manufacturer to have a B.E.T. surface area of 7 ± 2 m^2/g, and were measured in house as having a

BET surface area of 5.6 m^2/g. The average primary particle diameters (D_{BET}) of the powders were estimated from the B.E.T. surface areas (S_{BET}) and the powder densities (ρ) using the following equation[15]:

$$D_{BET} = 6 / (\rho * S_{BET}) \quad (1)$$

This approximation indicated that the NiO and YSZ average primary particle sizes were 240 nm and 180 nm, respectively.

The NiO and YSZ powders were ground together with a mortar and pestle in a ratio of 65 wt. % NiO to 35 wt. % YSZ. This powder was then dispersed in a mixed solvent system comprised of ~ 80 wt. % diacetone alcohol and ~ 20 wt. % alpha-terpineol. The dispersant Disperbyk 111 was also added (95 % active, BYK additives). The powder comprised ~ 10 wt. % of the ink and the dispersant was 2 - 5 wt. % of the powder. The following additional binders and plasticizers were added to simulate a real ink for usage in solid oxide fuel cell printing: ethyl cellulose binder (Dow, Ethocel Std. 300), polyvinyl butyral, polyalkylene glycol, and benzyl butyl phthalate. This formulation is similar to those in previously published SOFC printing studies[9]. A representative ink formulation is shown below (Table 1):

Table 1: Representative formulation of NiO/YSZ anode inks for SOFC printing

Component	Percentage by weight
NiO powder	6.5
YSZ powder	3.5
Diacetone alcohol	17.5
Alpha-terpineol	70.0
Disperbyk D111	0.4
Ethyl cellulose	0.2
Polyvinyl butyral	0.6
Benzyl butyl phthalate	0.6
Polyalkylene glycol	0.6

Ink Processing Equipment and Procedures

Four different ink processing protocols were investigated. The protocols consisted of combinations of low energy milling using a rolling mixer and high energy ball milling using a SPEX 8000M mixer mill. The low energy mixer rolls jars of ink at 60 rpm. The low energy mixing was carried out in an almost full glass jar, comprised of two thirds ink and one third YTZ grinding media (5 mm size, Tosoh). During high energy milling, the SPEX 8000M mixer mill shakes the ink container at a rate of approximately 1080 cycles per minute. High energy milling was carried out in a ceramic vial comprised of either magnesia-stabilized zirconia (SPEX) or alumina (SPEX). Two 13 mm zirconia beads were used as milling media.

High energy dry shaker milling refers to milling of the dry powders with the SPEX 8000M mixer mill. High energy slurry milling and dispersion refers to milling of the powders, solvent and dispersant with the SPEX 8000M mixer mill. All dry milling experiments were performed by charging the ceramic vessel with 10 grams of NiO/YSZ powder, and all slurry milling experiments were performed by charging the ceramic vessel with ~ 13 grams of powder and solvent. The percentage powder in the slurry milling experiments was 62 % by weight, which corresponds to ~ 20 % by volume. For processing protocols employing high energy slurry dispersion, the final ink was made by slowly dripping vehicle into the concentrated dispersion until the percentage of ceramic powder was reduced to 10 wt. %. Magnetic stirring was employed during the vehicle addition step. The resultant ink could then be stored under magnetic stirring or on the low energy rolling mill.

Analytical Techniques

The surface areas of the dry and degassed powders were measured via B.E.T. using a nitrogen adsorption technique (Micrometrics, ASAP 2020). The surface area of the unmilled YSZ powder measured with this machine was within the value specified by the manufacturer. Scanning electron microscopy (S.E.M.) images were obtained with a Jeol field emission scanning electron microscope. Dynamic light scattering measurements were obtained at a 90º detection angle using a Nicomp 300 ZLS. The measurements were performed by diluting the inks in a compatible solvent (2-butanol), sonicating the dilution for five minutes, and allowing the diluted sample temperature to stabilize at 25º C before measurement. Each sample underwent five sequential 10 minute measurements. The reported particle size distributions were constructed using the Nicomp fitting algorithm. All reported data have fit errors of less than 2.

Results

Effect of High Energy Dry Milling

In order to evaluate the effect of high energy dry milling on ink particle size, two different ink processing protocols were compared. Protocol 1 entailed placing the NiO and YSZ powders into a solvent/dispersant solution and dispersing for four hours via low energy mixing (on the 60 rpm rolling mill). Then, binders and plasticizers were added and the ink was returned to the low energy rolling mill for a total mixing time of five days. Protocol 2 entailed high energy shaker milling of the dry NiO and YSZ powders for 400 minutes then dispersing the powders and mixing the inks as described above for protocol 1.

Prior to dispersion, the surface area of the NiO/YSZ powder was evaluated as a function of high energy shaker milling time (Figure 1). The surface area increased linearly from 3.1 m^2/g for the unmilled powder to 12.2 m^2/g for the powder milled for 400 minutes. These surface areas correspond to a B.E.T. average primary particle size of ~ 300 nm for the unmilled NiO/YSZ powder and ~ 75 nm for the NiO/YSZ powder milled for 400 minutes. It is important to note that the initial B.E.T. surface area of the unmilled powder (3.1 m^2/g) is lower than what would have been expected based on the B.E.T. measurements of the individual powders (surface areas of 3.8 m^2/g for NiO and 5.6 m^2/g for YSZ). However, replicate B.E.T. measurements showed an error of ± 20 % which is ascribed to errors in measurement of the mass of the powder samples. Even acknowledging the error bars in the surface area measurements, significant particle size changes are evident with milling. Also, the surface area increases linearly with no apparent approach of an asymptote, indicating that additional milling would likely lead to even greater particle size reduction. Scanning electron microscopy images of the NiO/YSZ powder before milling and after 400 minutes of milling showed that the

milled powder possessed more sub 100 nm particles as compared to the unmilled powder (Figure 2). However, the S.E.M. images also indicated that the NiO/YSZ powder milled for 400 minutes still contained aggregates as well as primary particles greater than 1 μm.

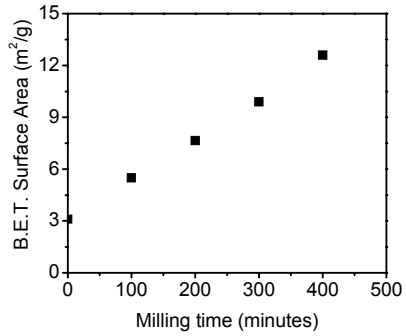

Figure 1: *Surface area of a 65:35 wt. % mixture of NiO/YSZ powder as a function of time spent on the SPEX 8000M high energy mill.*

Comparison of the number weighted particle size distributions of inks made via protocols 1 and 2 (Figure 3), showed that while both protocols resulted in a main peak at approximately 300 nm, the lack of milling in protocol 1 resulted in a bimodal distribution with a secondary peak at about 450 nm. This secondary peak was greatly diminished through the high energy milling step of protocol 2. The ink made via protocol 2 had 4 % dispersant as opposed to 2 % dispersant for the ink made via protocol 1. However, previous tests on inks made via protocol 1 indicated that the particle size distribution of these inks did not change when the dispersant percentage was increased from 1.5 % to 3% (data not shown). As such, the decrease in large size particles seen when following protocol 2 is ascribed to the high energy milling and not to the increased dispersant percentage.

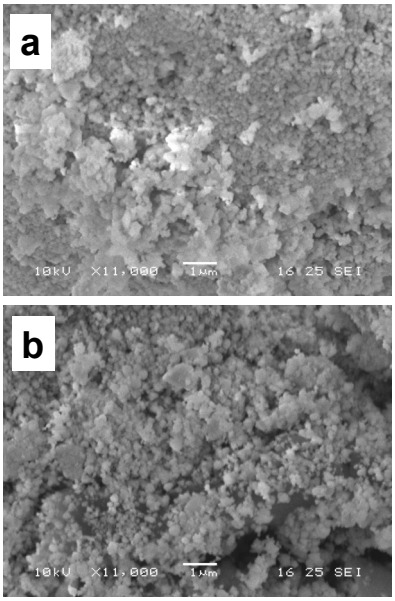

Figure 2: *Scanning electron microscopy images of a) NiO/YSZ powder before high energy dry milling, and b) after 400 minutes of high energy dry milling.*

Effect of high energy slurry milling

In a third ink processing protocol, high energy slurry milling replaced both low energy dispersion and high energy dry milling. For this protocol, a slurry of NiO/YSZ particles (62 wt. %), solvent and dispersant was milled for 135 minutes. Then additional vehicle (solvent, binders, and plasticizers) was dripped into the slurry to create an ink that had 10 wt. % ceramic powder. This ink was stirred overnight. The ink thus created was tested after approximately 18 hours with dynamic light scattering (Figure 4). Results showed that there was just one peak in the particle size distribution, and that the peak was centered at approximately 300 nm. In contrast, the ink created via protocol 1 and tested after 24 hours of dispersion showed a much broader particle size distribution. The primary peak was at approximately 300 nm, but there was a large tail indicating many particles between 300 nm and 1 μm.

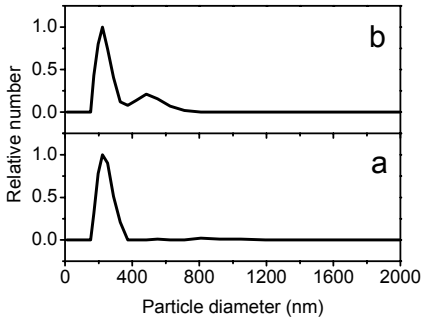

Figure 3: *Number weighted particle size distribution of NiO/YSZ ink formulated through* ***a)*** *a process that includes high energy shaker milling of the dry NiO/YSZ powder followed by low energy dispersion, and* ***b)*** *a process that includes only low energy dispersion. Both inks are tested after five days of low energy dispersion.*

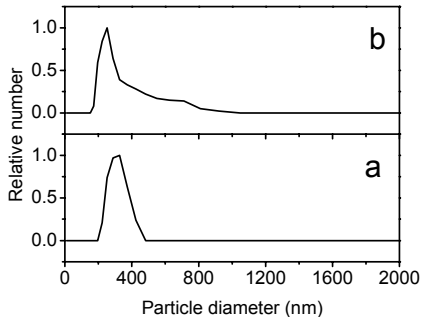

Figure 4: *Number weighted particle size distribution of NiO/YSZ ink formulated through* ***a)*** *a process that includes high energy dispersion of the NiO/YSZ powder followed by dilution with ink vehicle, and* ***b)*** *a process that includes only low energy dispersion. Both inks are tested after one day of processing. Ink created with protocol 3 was stored under continual magnetic stirring.*

Effect of combined high energy dry milling and high energy slurry dispersion

In a fourth ink processing protocol, 300 minutes of high energy dry milling preceded a similar slurry milling and vehicle dilution process as that described for protocol 3. Dynamic light

scattering measurements on inks produced by this fourth and final protocol showed a shift in the main peak from 300 nm down to less ~ 180 nm and also a decrease in the number of particles above 600 nm (Figure 5). This shift in the main peak from 300 nm to less than 180 nm distinguishes the fourth protocol as being effective not only for breaking up aggregates and large particles, but also for decreasing the size of even sub-300 nm particles.

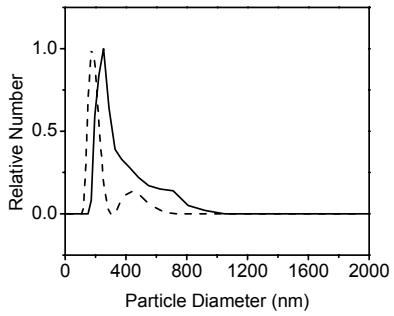

Figure 5: *Number weighted particle size distribution of NiO/YSZ ink produced using only low energy dispersion (solid line) and formulated through a process that includes high energy shaker milling of the NiO/YSZ powder followed by high energy slurry milling and subsequent dilution with ink vehicle (dashed line). The inks are tested after one day of processing. Ink produced via protocol 4 is stored on the low energy rolling mill after initial vehicle dilution.*

Discussion

Incorporating high energy dry shaker milling or high energy slurry dispersion into the ink making process resulted in an ink whose particle size distribution was narrower as compared to inks made via low energy dispersion. As could be seen from the particle size distributions of ink dispersed via low energy dispersion for five days, long term low energy dispersion breaks up some aggregates, but it does not eliminate all particles greater than 500 nm. It also does not decrease average particle size below initial powder primary particle sizes. In short, low energy dispersion may lead asymptotically to an ink whose particle size distribution reflects that of the initial powder, but not to any additional decrease in aggregate presence or primary particle size. This suggests that low energy dispersion is most appropriately employed for powders whose initial particle size distribution approximates the distribution desired in the ink. When a smaller primary particle size or lower degree of aggregation is desired, high energy dry shaker milling or high energy slurry milling may be necessary.

Of all of the protocols investigated, the one that resulted in the greatest shift in the ink particle size distribution peak was the protocol that paired high energy dry shaker milling with high energy slurry dispersion (protocol 4). However, it is important to note here that none of the high energy protocols (protocols 2, 3, 4) have been optimized. Process control factors like milling time, quantity of sample, % ceramic particles, quantity of milling media, shape of milling media, and size of milling media all may affect the final particle size distribution of a dispersion. The choice of solvent, choice of dispersant, and quantity of dispersant can also affect the final particle size distribution. As such, while this report provides evidence that the combination of high energy dry shaker milling and high energy slurry dispersion is the most promising path forward, single step high energy slurry dispersion may be equally promising if process control and chemical factors are optimized.

Even in the absence of process and chemical optimization, these results show how different methods of ink preparation can be used to tailor ink particle size distributions for lab scale inks. This study thus enables the exploration of the effect of ink particle size distribution on SOFC anode microstructure. All of the inks evaluated in this study have been successfully printed with a Dimatix Materials Printer (model DMP-2800, Fuji).

Conclusions

Three new protocols including high energy dry shaker milling and high energy slurry milling were used to create nanoscale NiO/YSZ inks with controlled particle size distributions. All of the high energy ink processing protocols achieved a narrower particle size distribution than what was achievable through low energy ink processing. The high energy protocols can be further optimized and used to print SOFC anodes whose microstructures may be manipulated through the manipulation of the ink particle size distribution and through tailored sintering protocols. It is expected that the ability to control the SOFC anode microstructure will enhance electrochemical performance.

References

[1] A. Kirubakaran, S. Jain, and R. K. Nema, "A review on fuel cell technologies and power electronic interface," Renew. Sust. Energ. Rev., 13, 2430 (2009).

[2] J. R. Wilson and S. A. Barnett, "Solid Oxide Fuel Cell Ni--YSZ Anodes: Effect of Composition on Microstructure and Performance," Electrochem. Solid St., 11, B181 (2008).

[3] L. Holzer, B. Münch, B. Iwanschitz, M. Cantoni, T. Hocker, and T. Graule, "Quantitative relationships between composition, particle size, triple phase boundary length and surface area in nickel-cermet anodes for Solid Oxide Fuel Cells," J. Power Sources, 196, 7076 (2011).

[4] C. M. An, J.-H. Song, I. Kang, and N. Sammes, "The effect of porosity gradient in a Nickel/Yttria Stabilized Zirconia anode for an anode-supported planar solid oxide fuel cell," J. Power Sources, 195, 821 (2010).

[5] Z. Wang, N. Zhang, J. Qiao, K. Sun, and P. Xu, "Improved SOFC performance with continuously graded anode functional layer," Electrochem. Commun., 11, 1120 (2009).

[6] H. Abe, K. Murata, T. Fukui, W. J. Moon, K. Kaneko, and M. Naito, "Microstructural control of Ni-YSZ cermet anode for planer thin-film solid oxide fuel cells," Thin Solid Films, 496, 49 (2006).

[7] K. Sato, H. Abe, T. Misono, K. Murata, T. Fukui, and M. Naito, "Enhanced electrochemical activity and long-term stability of Ni-YSZ anode derived from NiO-YSZ interdispersed composite particles," J. Eur. Ceram. Soc., 29, 1119 (2009).

[8] M. Mosiadz, R. Tomov, S. Hopkins, G. Martin, D. Hardeman, B. Holzapfel, and B. Glowacki, "Inkjet printing of $Ce_{0.8}Gd_{0.2}O_2$ thin films on Ni-5%W flexible substrates," J. Sol-Gel Sci. Techn., 54, 154 (2010).

[9] A. M. Sukeshini, R. Cummins, T. L. Reitz, and R. M. Miller, "Inkjet Printing of Anode Supported SOFC: Comparison of Slurry Pasted Cathode and Printed Cathode," Electrochem. Solid St., 12, B176 (2009).

[10] M. A. Sukeshini, R. Cummins, T. L. Reitz, and R. M. Miller, "Ink-Jet Printing: A Versatile Method for Multilayer Solid Oxide Fuel Cells Fabrication," J. Am. Ceram. Soc., 92, 2913 (2009).

[11] R. I. Tomov, M. Krauz, J. Jewulski, S. C. Hopkins, J. R. Kluczowski, D. M. Glowacka, and B. A. Glowacki, "Direct ceramic inkjet printing of yttria-stabilized zirconia electrolyte layers for anode-supported solid oxide fuel cells," J. Power Sources, 195, 7160 (2010).
[12] N. Yashiro, T. Usui, and K. Kikuta, "Application of a thin intermediate cathode layer prepared by inkjet printing for SOFCs," J. Eur. Ceram. Soc., 30, 2093 (2010).
[13] D. Young, A. M. Sukeshini, R. Cummins, H. Xiao, M. Rottmayer, and T. Reitz, "Ink-jet printing of electrolyte and anode functional layer for solid oxide fuel cells," J. Power Sources, 184, 191 (2008).
[14] M. Ni, M. K. H. Leung, and D. Y. C. Leung, "Micro-Scale Modeling of a Functionally Graded Ni-YSZ Anode," Chem. Eng. Technol., 30, 587 (2007).
[15] H. D. Jang, S.-K. Kim, and S.-J. Kim, "Effect of Particle Size and Phase Composition of Titanium Dioxide Nanoparticles on the Photocatalytic Properties," J. Nanopart. Res., 3, 141 (2001).

Author Biography

Jay Deiner received his BA in chemistry from Wesleyan University (1997) and his PhD in chemistry from Harvard University (2003). He has worked as a post doctoral fellow in electrochemistry at the University of São Paulo and as an ink formulation chemist at Hewlett-Packard. He is currently an assistant professor of Chemistry at the New York City College of Technology (CUNY) and a summer faculty fellow at the Air Force Research Labs.